SSRNet: Scalable 3D Surface Reconstruction Network

Zhenxing Mi [†]   Yiming Luo [†]   Wenbing Tao [*]

National Key Laboratory of Science and Technology on Multi-spectral Information Processing
School of Artifical Intelligence and Automation, Huazhong University of Science and Technology, China

{m201772503, yiming_luo, wenbingtao}@hust.edu.cn

Abstract

Existing learning-based surface reconstruction methods from point clouds are still facing challenges in terms of scalability and preservation of details on large-scale point clouds. In this paper, we propose the SSRNet, a novel scalable learning-based method for surface reconstruction. The proposed SSRNet constructs local geometry-aware features for octree vertices and designs a scalable reconstruction pipeline, which not only greatly enhances the predication accuracy of the relative position between the vertices and the implicit surface facilitating the surface reconstruction quality, but also allows dividing the point cloud and octree vertices and processing different parts in parallel for superior scalability on large-scale point clouds with millions of points. Moreover, SSRNet demonstrates outstanding generalization capability and only needs several surface data for training, much less than other learning-based reconstruction methods, which can effectively avoid overfitting. The trained model of SSRNet on one dataset can be directly used on other datasets with superior performance. Finally, the time consumption with SSRNet on a large-scale point cloud is acceptable and competitive. To our knowledge, the proposed SSRNet is the first to really bring a convincing solution to the scalability issue of the learning-based surface reconstruction methods, and is an important step to make learning-based methods competitive with respect to geometry processing methods on real-world and challenging data. Experiments show that our method achieves a breakthrough in scalability and quality compared with state-of-the-art learning-based methods.

1. Introduction

Point cloud is an important and widely used representation for 3D data. Surface reconstruction from point clouds (SRPC) has been well studied in computer graphics. A lot

---

[†]Equal contribution
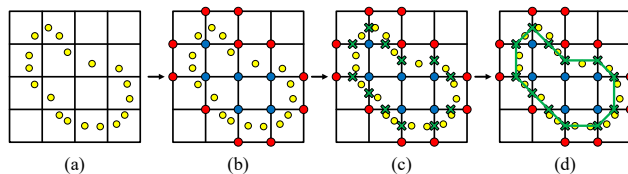[*]Corresponding author

Figure 1. 2D example of surface reconstruction methods using implicit function. Yellow dots represent points in point cloud. Red dots represent vertices outside the implicit surface. Blue dots represent vertices inside the implicit surface. According to the implicit function value on vertices, the MC method finds the intersections (green ×) of the grid lines and the implicit surface and then connects these intersections to extract a surface (green line).

of geometric reconstruction methods have been proposed [7, 4, 30, 15, 13, 11, 14, 2]. A commonly used pipeline in geometric reconstruction methods first computes an implicit function on a 3D grid [7, 14]. Then the Marching Cubes (MC) [17] is applied to extract an isosurface from the 3D grid through implicit function values. The grid is usually an adaptive octree. The intersection of two grid lines in an octree is named as octree vertex. Specifically, the implicit function can be an indicator function that indicates whether the vertices are inside or outside the implicit surface. That is, a surface reconstruction problem can be seen as a binary classification problem for octree vertices (See Figure 1).

In real-world reconstruction tasks, point clouds are mainly acquired by scanners or Multi-View Stereo (MVS) methods [26, 31] and are usually dense with more than millions of points and with complex topologies, which bring great challenges to surface reconstruction. With the development of deep learning, a variety of learning-based surface reconstruction methods have been proposed [8, 24, 16, 10, 19, 20]. However, there are still problems for them to reconstruct real-world point clouds for four reasons.

1) The network architectures and output representations of these learning-based methods usually force the learning-based methods to consider all the points at once. Therefore, they can not allow dividing input data and processing dif-
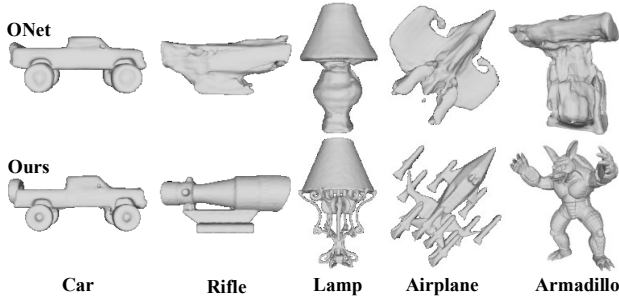
Figure 2. Examples of reconstructed surfaces of ONet [19] and Ours on ShapeNet [5] and Stanford 3D [27] (Armadillo).

ferent parts separately. When point clouds scale to millions of points, devices may not be able to handle large amounts of memory usage, which will make the model less scalable. For example, the Deep Marching Cubes [16] transforms the entire point cloud into voxel grids at once and directly outputs a irregular mesh, which is less scalable and only applicable to point clouds with thousands of points.

2) Although some methods can be applied to large-scale point clouds, in reality they greatly downsample or aggregate the points into a relative small scale. For example, the Occupancy Networks (ONet) [19] and DeepSDF [20] encode the entire points into a fixed-size latent vector of 512 elements, which greatly limits the representative power. Consequently, they come at the expense of surface quality reconstructed from large-scale point clouds.

3) Even on small-scale point clouds, the existing learning-based methods are good at reconstructing shapes with quite simple topology rather than those complex shapes. In fact, the result surfaces of simple shapes are usually over smoothed. The Figure 2 shows reconstruction examples of a state-of-the-art learning-based method (ONet) [19] and ours. For the simple shapes, ONet gets smooth surfaces. However, for the more complex topology shapes, it can not perfectly reconstruct the relevant details.

4) Some learning-based methods need a large portion of the dataset for training. For example, ONet uses 4/5 of its dataset (about $40K$ 3D shapes) as training set. Thus the network is inevitably more prone to over fitting the dataset. What's more, it can not generalize well among different datasets, while SSRNet needs only several surface data for trainning and the trained model on one dataset can be directly used on the other datasets with superior performance.

In this paper, we take the advantages of the commonly used implicit function method discussed above for surface reconstruction. Specifically, the implicit function values are 0-1 labels of octree vertices. They indicate whether the octree vertices are in front or at back of the implicit surface. The strategy simplifies the surface reconstruction to binary classification problem, which is simpler and more effective.

The ONet [19] also trains its network in a binary classification manner. However, this strategy does not guarantee high quality results. There are three main limitations in dealing with large-scale data that need to be broken.

1) **The scalability of the network.** A strong scalability of the classification network is important for tackling large-scale data. However, the commonly used PointNet [21] in reconstruction methods considers entire points at once and is thus less scalable. Our network does not need to input the entire data at once because the tangent convolution [28] operations involved in our network are all performed in a fixed-size local spatial region, and each 1×1 convolution operation is also independent. Moreover, these network operations are independent from the octree structures. Therefore, our network allows dividing the points and octree vertices through bounding boxes and processing different parts separately so that it wins strong scalability.

2) **The ability to reconstruct geometry details.** In order to achieve a high classification accuracy for octree vertices, the ability to capture local geometry details is essential. Some methods like ONet[19] and DeepSDF [20] aggregate the features of the entire points into a fixed-size global latent vector (512 elements), which lose a lot of geometry details. This will inevitably lead to a decrease on reconstruction quality. In our network, we focus on learning local geometry information of the implicit surface. Since the implicit surfaces are determined by octree vertex labels, in order to make accurate classification for octree vertices, the most important task is to construct vertex features properly. The octree vertex features in our network are constructed from local neighbor points and take the advantage of local projection information, such as the signed projection distances between octree vertices and their neighbor points, which are commonly used in geometric methods such as the TSDF [7] method and MLS methods [15, 11]. They enable our method to capture local geometry details of large-scale point clouds and directly provide local geometry information for accurate front-back classification. Therefore, our network benefits from geometry-aware features to reconstruct accurate surfaces. Some other methods such as the ONet[19] and DeepSDF [20] construct the features of vertices by directly concatenating 3D coordinates of vertices with the global latent vector of the point cloud. This feature construction method cannot provide explicit information about relative position between vertices and the implicit surface. Therefore, they cannot capture local geometry details well to reconstruct quality surfaces.

3) **The generalization ability of the network.** Paying too much attention to global feature rather than just considering local information would limit the generalization performance among different types of shapes. The octree vertex features in our network are local geometry-aware. They do not rely on global shape information excessively. There-

fore, it has good generalization capability and does not need too much training data, which avoids overfitting on dataset.

Overall, our contributions can be summarized as follows.

- We design a scalable pipeline for reconstructing surface from real-world point clouds.

- We construct local geometry-aware octree vertex feature, which leads to accurate classification for octree vertices and good generalization capability among different datasets.

Experiments have shown that our method achieves a significant improvement in scalability and quality compared with state-of-the-art learning-based methods, and is competitive with respect to state-of-the-art geometric processing methods in terms of reconstruction quality and efficiency [1].

2. Related Work

In this section, we first review some important geometric reconstruction methods to introduce basic concepts. Then we focus on existing learning-based surface reconstruction methods. We mainly analyze whether they are able to scale to large-scale datasets and to capture geometry details in terms of network architectures and output representations.

2.1. Geometric reconstruction methods

Geometric reconstruction methods can be broadly categorized into global methods and local methods. The global methods consider all the data at once, such as the radial basis functions (RBFs) methods [4, 30], and the (Screened) Poisson Surface Reconstruction method (PSR) [13, 14].

The local fitting methods usually define a truncated signed distance function (TSDF) [7] on a volumetric grid. The various moving least squares methods (MLS) fit a local distance field or vector fields by spatially varying low-degree polynomials, and blend several nearby points together [15, 11]. The local projection and local least squares fitting used by MLS are similar to the tangent convolution used in our network. Local methods can be well scaled.

There are also other geometric methods with different strategies, such as [2] computing restricted Voronoi cells. More detailed reviews and evaluations of geometric methods can be found in [1] and [32].

2.2. Learning-based reconstruction methods

Network architecture. One straightforward network architecture for point clouds is to convert the point clouds into regular 3D voxel grids or adaptive octree grids and apply 3D convolutions [18, 23]. The voxel-based network used in 3D-EPN [8] and the Deep Marching Cubes (DMC) [16] faces cubic growth of computation and memory requirements for large-scale datasets. The OctNetFusion [24] and 3D-CFCN [3] reconstruct implicit surface from multiple depth images based on OctNet [23], a octree-based network, whose operations are complicated and are highly related to the octree structure. Therefore, they also face computational issues in reconstructing large-scale datasets.

Another type of network architecture learns point features directly. The commonly used point cloud network is PointNet [21]. It encodes global shape features into a latent vector of fixed size. Some reconstruction methods also extract a latent vector from the point cloud, such as ONet [19] and DeepSDF [20]. These networks are able to encode features of a large-scale point cloud into a latent vector. However, the latent vector of a small size limits its representative power for complex point clouds.

There are also network architectures learning local features of point clouds. PointNet++ [22] groups points into overlapping parts, then PointNet is chosen as the local feature learner for each part. The centroids of each parts are selected using iterative farthest point sampling (FPS). The points are grouped around the centroids by ball query that finds all points within a radius to the query point. Using FPS with grouping operations cannot be guaranteed to be performed in a fixed-size spatial region. Therefore, the Point-Net++ does not allow dividing input points using bounding boxes and processing each part independently. The tangent convolution network [28] learns local features from neighbor points for semantic segmentation of 3D point clouds. It defines three new network operations: tangent convolution, pooling and unpooling. The neighbor points are collected by ball query. The pooling and unpooling are implemented via hashing onto a regular 3D grid. These operations are performed in a fixed-size spatial region. Therefore, the tangent convolution network can divide points using bounding boxes and process each part independently.

Output representation. The scalability of learning-based reconstruction methods is also greatly influenced by the output representation. The reconstruction methods based on voxel or octree grids usually use the occupancy or TSDF on grids as the output representation. This output representation, together with their network operations, is highly related to the grid structure. Therefore, their scalability is limited. The Deep Marching Cubes [16] and AtlasNet [10] directly produce a triangular surface. The predictions of different parts of the surface are interdependent so they have to consider the whole input point cloud at once.

ONet [19] and DeepSDF [20] learn shape-conditioned classifiers whose decision boundary is the surface. Their representations are similar to the front-back representation of our SSRNet. Although ONet and DeepSDF support to make predictions over 3D locations parallelly, they need to get the global latent vector of the whole point cloud so they do not allow dividing input points.

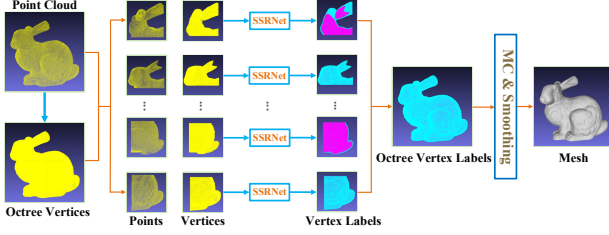[1]Our code will be available in Github later.

Figure 3. The pipeline of our method. Different parts are processed by our SSRNet parallelly.

3. Method

3.1. Pipeline

We design a scalable learning-based surface reconstruction method, named SSRNet, which allows dividing the input point clouds and octree vertices. Figure 3 shows the pipeline of our method. Let $\mathcal{P} = \{\mathbf{p}_i | i = 1, ..., N\}$ be the input point cloud of N points, where $\mathbf{p}_i$ is point coordinate with normal $\mathbf{n}_i$. We construct an octree from this point cloud and extract the vertices $\mathcal{V} = \{\mathbf{v}_i | i = 1, ..., M\}$ of the finest level of this octree, where each vertex $\mathbf{v}_i$ is the coordinate. To prevent the whole input data exceeding the GPU memory, we use bounding boxes to divide the point cloud and the vertices into $\{\mathcal{P}_j | j = 1, ..., K\}$ and $\{\mathcal{V}_j | j = 1, ..., K\}$, where K is the number of boxes. The bounding boxes of vertices are not overlapping. The corresponding bounding boxes of points are larger than those of octree vertices, which ensures that all the neighbor points needed by vertices are included in the input. The border effects are thus largely suppressed. This enables our network to make accurate predictions for vertices in the boundary of the bounding box. We do not see any decay of accuracy on the borders of vertex boxes. For the part j, the vertices $\mathcal{V}_j$ and the corresponding points $\mathcal{P}_j$ are fed into SSRNet. The SSRNet classifies each vertex $\mathbf{v}_{ji}$ in $\mathcal{V}_j$ as in front or at back of the implicit surface represented by $\mathcal{P}_j$. Let the function represented by the network be f_θ, where θ represents the parameters of the network. Then the key of our method is to classify $\mathbf{v}_{ji}$ in $\mathcal{V}_j$. It can be formulated as:

$$f_\theta(\mathcal{P}_j, \mathcal{V}_j, \mathbf{v}_{ji}) \rightarrow \{0, 1\} \tag{1}$$

The front or back of an vertex is defined by the normal direction of its nearest surface. The vertices are all from the finest-level voxels of the octree in order to reconstruct more details. They do not contain vertices far from the actual surface, which brings great challenges in classifying the vertices. It is worth noting that the network operations in SSRNet are not related to the structure of the octree. After all the vertices are labeled, we extract surface using Marching Cubes (MC) and post-process the surface with a simple Laplacian-based mesh smoothing method.

3.2. Geometry-aware Vertex Feature

As discussed in the Introduction, the most important features for octree vertex classification are signed projection distances among octree vertices and their neighbor points. In order to get accurate classification for octree vertices and good generalization capability, we design geometry-aware features for octree vertices directly encoding local projection information.

The tangent convolution [28] is defined as the 2D convolution on tangent images which are constructed by local projections of neighbor points. The indices of the projected points used for tangent image can be precomputed, which makes tangent convolution much more efficient. The signals used in tangent images represent local surface geometry, including signed projection distances, normals, etc. Therefore, it has the potential to encode local geometry features for octree vertices.

However, there are problems in applying tangent convolution to octree vertices directly. For a 3D location $\mathbf{p}$, the normal $\mathbf{n_p}$ of its tangent image is estimated through local covariance analysis [25]. Let $\mathbf{k}$ be the eigenvector related to the smallest eigenvalue of the covariance matrix of $\mathbf{p}$. The normal of tangent image is defined as $\mathbf{k}$. Due to the direction of eigenvector $\mathbf{k}$ is ambiguous, it may not be consistent with the real orientations of local implicit surfaces. The signs of projection distances hence do not represent front-back information accurately.

In order to solve this problem, we modify the definition of $\mathbf{n_p}$. Since the front-back classification is related to neighbor points, we use the input normals of neighbor points as additional constraints to define $\mathbf{n_p}$. Let $\mathbf{n}_a$ be the average input normal of the neighbor points of $\mathbf{p}$. In our definition, if the angle between eigenvector $\mathbf{k}$ and $\mathbf{n}_a$ is more than $90°$, we invert the direction of $\mathbf{k}$. Then we use it as the normal $\mathbf{n_p}$ of the tangent image. That is, our definition of the tangent image ensures that $\mathbf{n_p}^\top \mathbf{n}_a > 0$.

The features of octree vertices constructed by modified tangent convolution directly encode front-back information. They are local geometric features and not related to global information of shapes, so our network is scalable and can generalize well among different datasets. It's worth noting that we use neighbor points in the point cloud rather than neighbor vertices to compute the tangent images. It is because our network classifies octree vertices with respect to the surface represented by points from $\mathcal{P}$, rather than being represented by neighbor vertices.

3.3. Network

Network architecture. The network architecture of our SSRNet is illustrated in Figure 4. It contains two parts. The left part is for point feature extraction. The right is for vertex feature construction and label prediction. They are connected by tangent convolution layers for vertices.

The left part of our network encodes the features of the input N points from a point cloud. It is a fully-convolutional U-shaped network with skip connections. It is built by our modified tangent convolution layers. Two pooling operations are used to increase the size of the receptive field. The indices of the projected points used for tangent images and the index matrices used by pooling and unpooling layers are precomputed before the data are fed into the networks.

The right part is the core of our method. The geometry-aware features of octree vertices are firstly constructed by modified tangent convolution, from point features in corresponding scale levels. The indices of neighbors points from point cloud for tangent images of vertices are also precomputed before network operations. Then 1×1 convolutions and unpooling operations are applied to encode more abstract features and to predict labels for each vertex. The index matrices used by unpooling layers in this part are precomputed when downsampling vertices via grid hashing.

The input signals used by our method are all local signals. We use signed distances from neighbor points to the tangent plane (D), and normals relative to the normal of the tangent plane (N) as input. Since the network operations in SSRNet are all performed in a fixed-size local region, i.e. the modified tangent convolution, the 1×1 convolution, the pooling and unpooling of points and vertices, our network allows dividing the points and vertices with bounding-boxes and processing each part separately. It is worth noting that bounding boxes used for points are larger than those of octree vertices in order to make accurate predictions for vertices near the boundary.

Implementation details. In our implementation, we downsample the input points and vertices using grid hashing for pooling and unpooling. Given an octree of depth D, The length of the finest-level edges is $1/2^D$. We set the initial receptive field size in our network as $4/2^D$. The grid hashing size of input points at three scales are set as $1/2^{(D+2)}$, $1/2^{(D+1)}$, $1/2^D$. We do not apply gird hashing for vertices in the first scale because the vertices have an initial grid size of $1/2^D$ originally. The last two grid hashing sizes of vertices are set as $1/2^{(D-1)}$ and $1/2^{(D-2)}$. In order to retain more surface details for the feature construction of vertices, we set smaller grid hashing sizes for points.

3.4. Surface Extraction and Smoothing

We use MC [17] to extract surface from the labeled octree vertices. MC finds the intersections between octree edges and the implicit surface using the labels of vertices. Since we directly use the mid-points of edges as the intersections, the resulting mesh has discretization artifacts inevitably. We use a simple Laplacian-based smoothing method [29] as a post-processing step to refine the mesh.
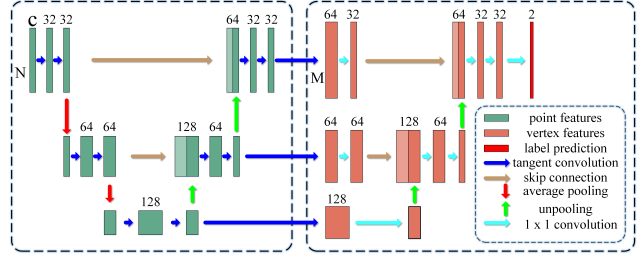

Figure 4. Our network architecture. Arrows of different colors represent different network operations. The inputs of this network include N points and M octree vertices. The initial features of the points have C channels.

3.5. Data Preparation

To prepare training data, we first normalize the coordinates of the input point cloud and surfaces. Then an octree is built from the point cloud. The octree building method is adapted from the open-source code of PSR [14]. It ensures that the finest level of the result octree contains not only cubes with points in them, but also their $3 \times 3 \times 3$ neighbor cubes. Therefore, the octree is dense enough to completely reconstruct the surface. We then use the ground truth surface with normals to label these vertices. For datasets without ground truth surfaces, we generate ground truth surfaces through PSR. More detailed introduction of our data preparing method can be found in our supplementary file.

4. Experiments

In this section we perform a series of experiments on datasets of different scales to evaluate our method. The datasets are all widely used in 3D-related tasks. We mainly examine the ability to capture geometry details, the scalability and generalization capability of our method on both small-scale and large-scale datasets. Due to the lack of triangular meshes, the ground-truth meshes used for training are all produced by PSR. It is worth noting that we just get ground-truth labels from the triangular surfaces produced by PSR in the experiments due to the lack of public available large-scale surface datasets. However, our labels are not only available from PSR.

4.1. Datasets and Evaluation Metrics

Datasets. In order to compare with several state-of-the-art learning-based methods, we do experiments on the same subset of ShapeNet [5] as ONet [19], in which the point clouds are relatively small with tens of thousands of points in each. Furthermore, in order to better evaluate the scalability and generalization capability to handle large-scale point clouds, we choose DTU dataset [12] and Stanford 3D Scanning Repository [27]. Most point clouds in the two datasets contain millions of points.
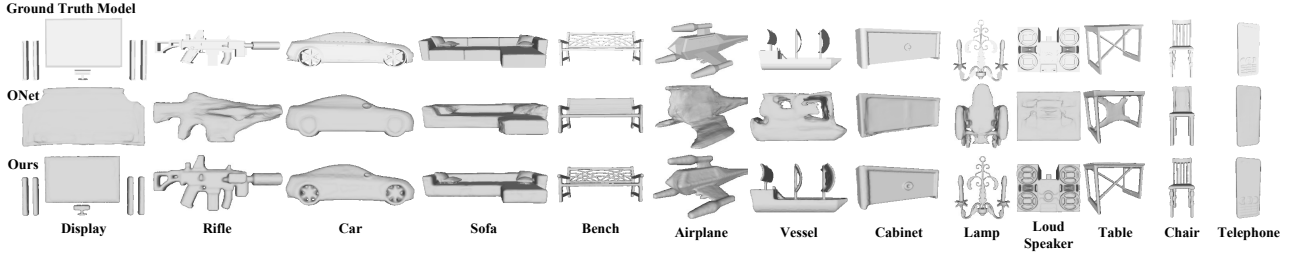
Figure 5. Examples of reconstructed surfaces on testing set of ShapeNet [5] by ONet [19] and our method.

Table 1. Classification Accuracy of SSRNet on Datasets of different scales. ShapeNet-Model and DTU-Model represent the models we trained on ShapeNet [5] and DTU [12] respectively.

Dataset	ShapeNet [5]	DTU [12]	Stanford [27]	
			ShapeNet-Model	DTU-Model
Accuracy (%)	97.6	95.7	98.1	98.2

Evaluation Metrics. The direct metric of our network is the classification accuracy of octree vertices. It is worth mentioning that the vertices in our experiments are all from the finest-level voxels of the octree. With octree of relatively high resolution, these voxels do not contain vertices very far from the actual surface. Therefore, a high classification accuracy matters a lot to the quality of the final mesh. For mesh comparison on ShapeNet, we use the same evaluation metrics with ONet, including the volumetric IoU (higher is better), the Chamfer-L_1 distance (lower is better) and the normal consistency score (higher is better). On the DTU dataset, we use DTU evaluation method [12], which mainly evaluates DTU Accuracy and DTU Completeness (both lower is better). And for Stanford datasets, Chamfer distance (CD) (lower is better) is adopted in order to evaluate the points of the output meshes, and the CD is also taken into consideration in the evaluation on DTU dataset. For each point in a cloud, CD finds the nearest point in the other point cloud, and averages the square of distances up.

4.2. Results on Shapenet

In our first experiment, we evaluate the capacity of our network to capture shape details on ShapeNet. We use the same test split as ONet for fair comparisons. The testing set contains about $10K$ shapes. We only randomly select a subset from the training set of ONet for training. The training set of our method ($4K$ shapes) is 1/10 of the training set of ONet ($40K$ shapes). We do not use a large amount of training data as ONet did mainly for two reasons. On the one hand, it is necessary to eliminate the possibility of overfitting a dataset due to too much training data. On the other hand, our network learns local geometry-aware features so that it can capture more geometry details with less training

data. Therefore, it is unnecessary for us to use too many training samples.

In our experiments, each point cloud in training and testing set contains $100K$ points. We add Gaussian noise with zero mean and standard deviation 0.05 to the point clouds as ONet did. Our network is efficient at processing point clouds with a large number of points, so we do not downsample the point clouds. We think it is important for Surface Reconstruction from Point Clouds (SRPC) methods to be adaptive to the original data, rather than reducing the amount of input data and the resolution to fit their networks. After all, the representative power of 300 points used by ONet is really limited. The original synthetic models of ShapeNet do not have consistent normals so that we reconstruct surfaces from the ground truth point clouds using PSR on octrees of depth 9 to generate the training data. We use octrees of depth 8 in SSRNet for training and testing.

For mesh comparison, we use the evaluation metrics on ShapeNet mentioned in Section 4.1, including the volumetric IoU, the Chamfer-L_1 distance and the normal consistency score. We evaluate all shapes in the testing set on these metrics. The results of existing learning based 3D reconstruction approaches, i.e. the 3D-R2N2 [6], PSGN [9], Deep Marching Cubes (DMC) [16] and ONet [19], are obtained from the paper of ONet. As mentioned in ONet, it is not possible to evaluate the IoU for PSGN for the reason that it does not yield watertight meshes. ONet adapted 3D-R2N2 and PSGN for point cloud input by changing the encoders. Although methods in Table 2 use different strategies, they actually solve the same task of SRPC. Quantitative results are shown in Table 2.

The classification accuracy of octree vertices on ShapeNet dataset shows strong robustness of our network. It achieves high classification accuracy of 97.6% on noisy point clouds (See Table 1). The Table 2 shows that our method gets great improvements on these metrics. Compared with the best performance of other methods, we achieve the highest IoU, lower Chamfer-L_1 distance and higher normal consistency. More specifically, the IoU of our results is about 18% higher than that of ONet. It is worth noting that our network has only 0.49 million parameters,

Table 2. Results of learning-based methods on ShapeNet [5]. NC = Normal Consistency. The volumetric IoU (higher is better), the Chamfer-L_1 distance (lower is better) and NC (higher is better) are reported.

	IoU	Chamfer-L_1	NC
3D-R2N2 [6]	0.565	0.169	0.719
PSGN [9]	–	0.202	–
DMC [16]	0.647	0.117	0.848
ONet [19]	0.778	0.079	0.895
Ours	**0.957**	**0.024**	**0.967**

Table 3. Surface quality on DTU [12] testing scenes. Surfaces used for evaluation criterias are all reconstructed at octree depth 9. DA=DTU Accuracy, DC=DTU Completeness, CD=Chamfer distance (all lower is better).

Method	DA		DC		CD	
	Mean	Var.	Mean	Var.	Mean	RMS
PSR(trim 8) [14]	0.473	1.33	0.327	0.220	3.16	12.5
PSR(trim 9.5) [14]	0.330	0.441	0.345	0.438	**1.17**	4.49
Ours	**0.321**	**0.285**	**0.304**	**0.0888**	1.46	**4.42**

Table 4. Generalization on Stanford 3D [27].The Chamfer Distances are in units of 10^{-6}. Surfaces used for distance criterias are all reconstructed at octree depth 9. Ours-S and Ours-D represent the models we trained on ShapeNet [5] and DTU [12] respectively.

Data	Accuracy(%)		CD Mean			CD RMS		
	Ours S	Ours D	ONet [19]	Ours S	Ours D	ONet [19]	Ours S	Ours D
Armadillo	98.2	97.8	93.46	0.028	**0.023**	168.59	0.131	**0.056**
Bunny	98.2	98.7	94.88	0.064	**0.057**	165.44	0.134	**0.087**
Dragon	98.0	98.0	40.69	0.053	**0.047**	74.99	0.208	**0.150**

while ONet has about 13.4 million parameters.

As shown in Figure 5, the surface quality of ours is generally better than those of ONet. Our network is good at capturing local geometry details of shapes of different classes, even with quite different and complex topology. ONet can reconstruct smooth surfaces for shapes with simple topology. However, since the global latent vector encoder in ONet loses shape details, it tends to generate an over-smoothed shape for a complex topology. For more visual results, please see our supplementary materials.

4.3. Results on 3D Scans of Larger Scales

Evaluation on DTU dataset. We train and test our network on DTU at octree depth 9. Since the ground truth surfaces of DTU are not available, we reconstruct surfaces using PSR at octree depth 10 to generate training data. We trim PSR surfaces using SurfaceTrimmer software provided in PSR with trimming value 8. We randomly extract batches of points from each training scene to train our network. Even though we use only 6 scenes in training set, we achieve a high accuracy and good generalization capability. Table 3 gives

Table 5. The time performance of our method. We report the first scale point number, first scale octree vertex number and triangle number in our results using million (M) as unit. The preprocessing time (Prep. time) includes octree construction time, downsampling time, tangent images precomputing time and batches computing time. The prediction time (Pred. time) is the time for loading partitioned points and vertices and predicting labels.

Number	Armadillo	Bunny	Dragon	stl_030	stl_034	stl_062
Point /M	2.16	0.361	1.71	2.43	2.01	2.19
Vertex /M	3.29	3.62	3.07	1.07	0.766	0.922
Triangle /M	1.18	1.52	1.16	0.42	0.31	0.36
Batch	109	73	77	59	88	86

Time /s	Armadillo	Bunny	Dragon	stl_030	stl_034	stl_062
Prep	19.4	8.86	16.6	10.9	9.34	9.99
Pred (1 GPU)	133	82.2	110.5	63.5	84.5	87.9
Pred (4 GPUs)	**50.5**	**27.3**	**38.2**	30.4	31.1	34.3
Total (1 GPU)	153	92.0	128	75.4	94.5	98.6
Total (4 GPUs)	**70.6**	**37.1**	**55.7**	42.3	41.1	45.0

the quantitative results on testing scenes in DTU dataset [2]. Qualitative results are shown in Figure 6 (a).

The point clouds in DTU are all open scenes. Although ONet can finish reconstruction tasks of watertight surfaces, it cannot reconstruct surface from point clouds of open scenes. Here we set results of PSR as an evaluation reference. Surfaces reconstructed by PSR for evaluation are also reconstructed at octree depth 9. The results of PSR are always closed surfaces even reconstructed from open scenes. Therefore, we trim them with trimming value 8 and 9.5.

As illustrated in Table 1, our network gets a high average classification accuracy of 95.7%. As Table 3 shows, compared with PSR with trimming value 8, our surfaces perform better on DTU Accuracy, DTU Completeness and CD. As for PSR with trimming value 9.5, we get similar performance on DTU Accuracy and perform better on DTU Completeness. The PSR with trimming value 9.5 is more accurate on CD while it is at cost of completeness. Our method differs from PSR that our method directly produces open surfaces and we do not need to apply a trimming step for our results, so we get more accurate and complete borders than PSR (See Figure 6 (a)). In conclusion, the quality of our method is comparable with PSR on DTU datasets. We perform better with respect to the completeness on open scenes. Detailed figures and videos are also provided in our supplementary materials.

4.4. Generalization Capability

In this section we evaluate the generalization capability of our method. It is worth noting that three datasets (ShapeNet, DTU, Stanford 3D) are quite different in terms of data scale and data category. Data in the ShapeNet are all

---

[2] We use scenes {1, 2, 3, 4, 5, 6} as training set, scenes {7, 8, 9} as validation set and scenes {10, 11, 12, 13, 14, 15, 16, 18, 19, 21, 24, 29, 30, 34, 35, 38, 41, 42, 45, 46, 48, 51, 55, 59, 60, 61, 62, 63, 65, 69, 84, 93, 94, 95, 97, 106, 110, 114, 122, 126, 127, 128} as testing set.

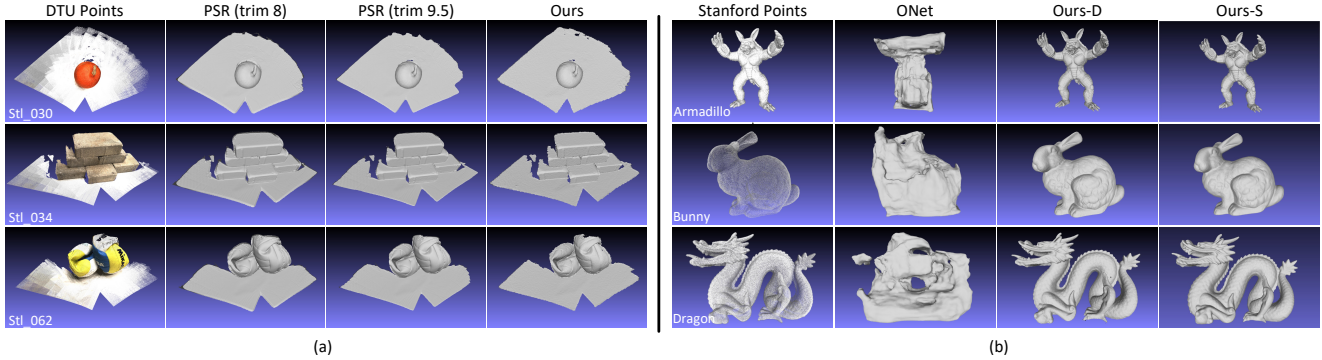| DTU Points | PSR (trim 8) | PSR (trim 9.5) | Ours | Stanford Points | ONet | Ours-D | Ours-S |

Figure 6. Examples of surfaces of our method and PSR [14] on DTU [12] (a). Generalization testing results of our method and ONet [19] on Stanford 3D [27] (b). Ours-S and Ours-D represent the our models trained on ShapeNet [5] and DTU [12] respectively. Background colors are for better visualization for point clouds.

synthetic. The DTU only contains real-world scan data of open scenes while the Stanford 3D only has closed scenes. Therefore, tests among these three datasets can well evaluate the generalization performance of SSRNet.

We test two trained models (SSRNet and ONet trained on ShapeNet) on Stanford 3D. Table 1 and Table 4 show that we achieve high average classification accuracy of 98.1%. SSRNet generalizes better than ONet on Stanford 3D in metric of Chamfer Distance. Figure 6 (b) shows that our results achieve outstanding visual effects and reconstruct geometry details of the shapes well.

We also use SSRNet model trained on DTU to test on Stanford 3D. Table 4 shows that our network trained on open scenes can also achieve higher classification accuracy on closed scenes. Besides, classification accuracy of our models trained on ShapeNet and DTU are almost exactly the same, and the evaluation results on CD are also similar. In general, the results prove good generalization capability of our network. One strong benefit is that we do not need to retrain our network on different datasets to complete the reconstruction work.

4.5. Efficiency

We test our network on 4 GeForce GTX 1080 Ti GPUs in a Intel Xeon(R) CPU system with 32×2.10 GHz cores. We implement data preprocessing method with CUDA. In our experiments, we set the maximum number of point and vertex in one batch as 300,000. As is illustrated in Table 5, our method can tackle millions of points and vertices in reasonable time [3]. As a learning-based method, the time consumption is generally acceptable. Since our network is able to perform predictions parallelly using multi-GPUs, our prediction procedure can be accelerated by more GPUs. As

shown in the table, the predictions with 4 GPUs are about 2.6 times faster than 1 GPU. This reveals the efficiency potential of our method scaling to large datasets. When conditions permitting (more GPUs), it can be accelerated a lot.

5. Conclusion

Our SSRNet has many advantages. Firstly, it has strong scalability that allows dividing the input data and processing different parts parallelly. Meanwhile, the network has also proved its efficiency by experiements in which it reconstructs quality surfaces from point clouds with millions of points in reasonable time. Besides, SSRNet is good at reconstructing geometry details with the help of the geometry-aware features. These features are only related to local neighbor information and do not rely on any global shape information. Paying too much attention to global shape feature rather than just considering local geometry information would limit the generalization capability among different shape types. Thus SSRNet also has good generalization capability and it does not need too much training data, which avoids overfitting.

In conclusion, we have successfully designed a scalable network for quality surface reconstruction from point clouds and make a significant breakthrough compared with existing state-of-the-art learning-based methods. We believe it would be an important step to make learning-based methods competitive with respect to geometry processing algorithms on real-world and challenging data.

Acknowledgements

---

[3]DTU [12] contains a series of point clouds, here we just randomly list time consumption of stl_030, stl_034, stl_062. We do not consider the time of reading and writing files.

References

[1] Matthew Berger, Andrea Tagliasacchi, Lee Seversky, Pierre Alliez, Joshua Levine, Andrei Sharf, and Claudio Silva. State of the art in surface reconstruction from point clouds. 2014. 3

[2] Dobrina Boltcheva and Bruno Lévy. Surface reconstruction by computing restricted voronoi cells in parallel. *Computer-Aided Design*, 90:123–134, 2017. 1, 3

[3] Yan-Pei Cao, Zheng-Ning Liu, Zheng-Fei Kuang, Leif Kobbelt, and Shi-Min Hu. Learning to reconstruct high-quality 3d shapes with cascaded fully convolutional networks. In *Proceedings of the European Conference on Computer Vision (ECCV)*, pages 616–633, 2018. 3

[4] Jonathan C Carr, Richard K Beatson, Jon B Cherrie, Tim J Mitchell, W Richard Fright, Bruce C McCallum, and Tim R Evans. Reconstruction and representation of 3d objects with radial basis functions. In *Proceedings of the 28th annual conference on Computer graphics and interactive techniques*, pages 67–76. ACM, 2001. 1, 3

[5] Angel X Chang, Thomas Funkhouser, Leonidas Guibas, Pat Hanrahan, Qixing Huang, Zimo Li, Silvio Savarese, Manolis Savva, Shuran Song, Hao Su, et al. Shapenet: An information-rich 3d model repository. *arXiv preprint arXiv:1512.03012*, 2015. 2, 5, 6, 7, 8

[6] Christopher B Choy, Danfei Xu, JunYoung Gwak, Kevin Chen, and Silvio Savarese. 3d-r2n2: A unified approach for single and multi-view 3d object reconstruction. In *European conference on computer vision (ECCV)*, pages 628–644. Springer, 2016. 6, 7

[7] Brian Curless and Marc Levoy. A volumetric method for building complex models from range images. 1996. 1, 2, 3

[8] Angela Dai, Charles Ruizhongtai Qi, and Matthias Nießner. Shape completion using 3d-encoder-predictor cnns and shape synthesis. In *Proceedings of the IEEE Conference on Computer Vision and Pattern Recognition (CVPR)*, pages 5868–5877, 2017. 1, 3

[9] Haoqiang Fan, Hao Su, and Leonidas J Guibas. A point set generation network for 3d object reconstruction from a single image. In *Proceedings of the IEEE Conference on Computer Vision and Pattern Recognition (CVPR)*, pages 605–613, 2017. 6, 7

[10] Thibault Groueix, Matthew Fisher, Vladimir G Kim, Bryan C Russell, and Mathieu Aubry. A papier-mâché approach to learning 3d surface generation. In *Proceedings of the IEEE Conference on Computer Vision and Pattern Recognition (CVPR)*, pages 216–224, 2018. 1, 3

[11] Gaël Guennebaud and Markus Gross. Algebraic point set surfaces. In *ACM Transactions on Graphics (TOG)*, volume 26, page 23. ACM, 2007. 1, 2, 3

[12] Rasmus Jensen, Anders Dahl, George Vogiatzis, Engil Tola, and Henrik Aanæs. Large scale multi-view stereopsis evaluation. In *2014 IEEE Conference on Computer Vision and Pattern Recognition*, pages 406–413. IEEE, 2014. 5, 6, 7, 8

[13] Michael Kazhdan, Matthew Bolitho, and Hugues Hoppe. Poisson surface reconstruction. In *Proceedings of the fourth Eurographics symposium on Geometry processing*, volume 7, 2006. 1, 3

[14] Michael Kazhdan and Hugues Hoppe. Screened poisson surface reconstruction. *ACM Transactions on Graphics (ToG)*, 32(3):29, 2013. 1, 3, 5, 7, 8

[15] David Levin. Mesh-independent surface interpolation. In *Geometric modeling for scientific visualization*, pages 37–49. Springer, 2004. 1, 2, 3

[16] Yiyi Liao, Simon Donné, and Andreas Geiger. Deep marching cubes: Learning explicit surface representations. In *Proceedings of the IEEE Conference on Computer Vision and Pattern Recognition (CVPR)*, pages 2916–2925, 2018. 1, 2, 3, 6, 7

[17] William E Lorensen and Harvey E Cline. Marching cubes: A high resolution 3d surface construction algorithm. In *ACM siggraph computer graphics*, volume 21, pages 163–169. ACM, 1987. 1, 5

[18] Daniel Maturana and Sebastian Scherer. Voxnet: A 3d convolutional neural network for real-time object recognition. In *2015 IEEE/RSJ International Conference on Intelligent Robots and Systems (IROS)*, pages 922–928. IEEE, 2015. 3

[19] Lars Mescheder, Michael Oechsle, Michael Niemeyer, Sebastian Nowozin, and Andreas Geiger. Occupancy networks: Learning 3d reconstruction in function space. In *Proceedings of the IEEE Conference on Computer Vision and Pattern Recognition*, pages 4460–4470, 2019. 1, 2, 3, 5, 6, 7, 8

[20] Jeong Joon Park, Peter Florence, Julian Straub, Richard Newcombe, and Steven Lovegrove. Deepsdf: Learning continuous signed distance functions for shape representation. In *Proceedings of the IEEE Conference on Computer Vision and Pattern Recognition*, pages 165–174, 2019. 1, 2, 3

[21] Charles R Qi, Hao Su, Kaichun Mo, and Leonidas J Guibas. Pointnet: Deep learning on point sets for 3d classification and segmentation. In *Proceedings of the IEEE Conference on Computer Vision and Pattern Recognition (CVPR)*, pages 652–660, 2017. 2, 3

[22] Charles Ruizhongtai Qi, Li Yi, Hao Su, and Leonidas J Guibas. Pointnet++: Deep hierarchical feature learning on point sets in a metric space. In *Advances in Neural Information Processing Systems*, pages 5099–5108, 2017. 3

[23] Gernot Riegler, Ali Osman Ulusoy, and Andreas Geiger. Octnet: Learning deep 3d representations at high resolutions. In *Proceedings of the IEEE Conference on Computer Vision and Pattern Recognition (CVPR)*, pages 3577–3586, 2017. 3

[24] Gernot Riegler, Ali Osman Ulusoy, Horst Bischof, and Andreas Geiger. Octnetfusion: Learning depth fusion from data. In *2017 International Conference on 3D Vision (3DV)*, pages 57–66. IEEE, 2017. 1, 3

[25] Samuele Salti, Federico Tombari, and Luigi Di Stefano. Shot: Unique signatures of histograms for surface and texture description. *Computer Vision and Image Understanding*, 125:251–264, 2014. 4

[26] Johannes L Schönberger, Enliang Zheng, Jan-Michael Frahm, and Marc Pollefeys. Pixelwise view selection for unstructured multi-view stereo. In *Proceedings of the European Conference on Computer Vision (ECCV)*, pages 501–518. Springer, 2016. 1

[27] Stanford 3D. The stanford 3d scanning repository, 2013. 2, 5, 6, 7, 8

[28] Maxim Tatarchenko, Jaesik Park, Vladlen Koltun, and Qian-Yi Zhou. Tangent convolutions for dense prediction in 3d. In *Proceedings of the IEEE Conference on Computer Vision and Pattern Recognition (CVPR)*, pages 3887–3896, 2018. 2, 3, 4

[29] Gabriel Taubin. A signal processing approach to fair surface design. In *Proceedings of the 22nd annual conference on Computer graphics and interactive techniques*, pages 351–358. ACM, 1995. 5

[30] Greg Turk and James F O'Brien. Modelling with implicit surfaces that interpolate. *ACM Transactions on Graphics (TOG)*, 21(4):855–873, 2002. 1, 3

[31] Qingshan Xu and Wenbing Tao. Multi-scale geometric consistency guided multi-view stereo. In *The IEEE Conference on Computer Vision and Pattern Recognition (CVPR)*, June 2019. 1

[32] Lingli Zhu, Antero Kukko, Juho-Pekka Virtanen, Juha Hyyppä, Harri Kaartinen, Hannu Hyyppä, and Tuomas Turppa. Multisource point clouds, point simplification and surface reconstruction. *Remote Sensing*, 11(22):2659, 2019. 3